Wadi Alshatti University Journal of Pure and Applied Sciences

مجلة جامعة وادي الشاطئ للعلوم البحتة والتطبيقية

Volume 4, No. 2, July-Decemer 2026 Online ISSN: 3006-0877 المجلد 4، الاصدار 2، يوليو- ديسمبر 2026

RESEARCH PAPER MATERIALS AND METALLURGICAL ENGINEERING

Influence of Cathodic Polarization on Passive Film and Corrosion Behavior of 2205 Duplex Stainless Steel in 0.9% wt. NaCl

Hesham Mraied[1,*], Fatima Alezmirly[1], Rayan Almahrug[2]

[1]Department of Materials and Metallurgical Engineering, University of Tripoli, Tripoli, Libya
[2]Faculty of Engineering, South Mediterranean University, Tripoli, Libya

ARTICLE HISTORY
Received 12 May 2026
Revised 03 Jun 2026
Accepted 10 Jun 2026
Online 20 Jun 2026

KEYWORDS
Duplex Stainless Steel;
Passive Film;
Electrochemical Impedance Spectroscopy;
Mott-Schottky;
Cathodic Polarization;
Corrosion Resistance.

ABSTRACT

The influence of cathodic polarization on the electrochemical behavior of the passive film of stainless steels in physiological environments is significant. In such environments, hydrogen interactions and electrochemical modifications of this passive layer can directly affect the corrosion resistance and durability of these alloys. Although cathodic polarization has been widely studied regarding its effects on hydrogen embrittlement and stress corrosion cracking in 2205 Duplex Stainless Steel, the impact of such conditions on the electrical properties of the passive layer in physiological environments is inadequately researched. In this research the effects of cathodic polarization on the behavior of the passive film of 2205 duplex stainless steel in a 0.9% wt. NaCl solution were investigated. Electrochemical Impedance Spectroscopy and Mott-Schottky analysis were used to study passive film stability, semiconductor properties, and corrosion resistance. Results revealed that cathodic polarization introduced hydrogen into the passive film, decreasing the flat band potential to –0.08 V vs. Ag/AgCl, as well as increasing the donor density to $3.6x10^{20}$ cm^{-3}. Electrochemical impedance spectroscopy suggested that the charge transfer resistance decreased, which is in good agreement with the passivity decay suggested by Mott-Schottky analysis. However, film thickness (1.9 nm) did not change, suggesting an electronic rather than structural changes in the passive film due to cathodic polarization. These findings highlighted the importance of understanding the trade-off between corrosion mitigation and hydrogen-induced film damage that might result from improper cathodic polarization practices.

تأثير الاستقطاب الكاثودي على سلوك الطبقة السلبية للفولاذ الغير قابل للصدأ (2205 ثنائي الطور) في محلول كلوريد الصوديوم 0.9% وزن

هشام المريض [1،*]، فاطمة الازمرلي [1]، ريان المحروق [2]

الكلمات المفتاحية

الفولاذ الغير قابل للصدأ ثنائي القطب
التحليل الطيفي للمقاومة الكهروكيميائية
تحليل موت–شوتكي
الاستقطاب الكاثودي
مقاومة التآكل

الملخص

يُعدّ تأثير الاستقطاب الكاثودي على السلوك الكهروكيميائي للغشاء السلبي في الفولاذ الغير قابل للصدأ في البيئات الفسيولوجية تأثيرًا مهمًا. ففي مثل هذه البيئات، يمكن لتفاعلات الهيدروجين والتعديلات الكهروكيميائية في هذه الطبقة أن تؤثر بشكل مباشر على مقاومة التآكل ومتانة هذه السبائك. على الرغم من أن الاستقطاب الكاثودي قد دُرس على نطاق واسع فيما يتعلق بتأثيره على التقصف الهيدروجيني والتشقق الناتج عن التآكل الإجهادي في الفولاذ الغير قابل للصدأ 2205 ثنائي الطور، فإن تأثير هذه الظروف على الخصائص الكهربائية للطبقة السلبية في البيئات الفسيولوجية لا يزال غير مدروس بشكل كافٍ. في هذا البحث، تم دراسة تأثيرات الاستقطاب الكاثودي على سلوك الغشاء السلبي لفولاذ الدوبلكس الغير قابل للصدأ (2205) في محلول كلوريد الصوديوم بتركيز **0.9%** وزن، وقد استُخدمت تقنيتا التحليل الطيفي للمقاومة الكهروكيميائية وتحليل موت–شوتكي لدراسة استقرار الغشاء السلبي، وخصائص أشباه الموصلات ومقاومة التآكل. أظهرت النتائج أن الاستقطاب الكاثودي أدخل الهيدروجين إلى الغشاء السلبي، مما قلل من جهد النطاق المسطح إلى سالب 0.08 فولت مقابل قطب فضة\كلوريد الفضة، بالإضافة إلى زيادة كثافة المادة المانحة إلى $3.6x10^{2}$ جرام\سم^{3}. اقترح التحليل الطيفي للمقاومة الكهروكيميائية أن مقاومة نقل الشحنة انخفضت، وهو ما يتوافق جيدًا مع الانحلال السلبي الذي اقترحه تحليل موت شوتكي. ومع ذلك، لم يتغير سمك الغشاء (1.9 نانومتر)، مما يشير إلى تغييرات إلكترونية وليست هيكلية في الغشاء السلبي بسبب الاستقطاب الكاثودي. سلطت هذه النتائج الضوء على أهمية فهم المفاضلة بين تخفيف التآكل وتلف الأغشية الناجم عن الهيدروجين والذي قد ينجم عن ممارسات الاستقطاب الكاثودي غير السليمة.

Introduction

Duplex Stainless Steel 2205 (DSS 2205) is an important classof engineering materials. It merges the desired properties of both austenitic and ferritic stainless steels. The chemicalcomposition of the alloy is approximately 22% chromium, 5% nickel, 3% molybdenum, and 0.17%

*Corresponding author
https://doi.org/10.63318/waujpasv4i2_02
This work is licensed under a Creative Commons Attribution-NonCommercial 4.0 International License (CC BY-NC 4.0).

nitrogen. The microstructure contains roughly equal amounts of austenite (γ) and ferrite (α) phass [1]. This dual-phase structure provides excellent mechanical strength where the yield strength equals twice of that of austenitic stainless steels, while good toughness and ductility are still maintained [2].

When compared to austenitic grades, DSS 2205 exhibits better corrosion resistance in different environments such as chloride enriched ones [3]. This is attributed to the high chromium and molybdenum content in the ferrite phase, as well as to the presence of nitrogen in the austenite phase. The alloy exhibits excellent resistance to both pitting and crevice corrosion, with a pitting resistance equivalent number (PREN) larger than 35 [4]. The passive film of DSS 2205 also contains high amounts of chromium and molybdenum oxides which provide the alloy with strong protection against corrosion. When aggressive anions (e.g., Cl^-) adsorb at weak points the passive film could break down, resulting in local pits initiation [5].

In high-temperature chloride or sulfide containing environments, DSS 2205 is prone to stress corrosion cracking (SCC) though its resistance is still better than that of 304L stainless steel [6]. In physiological environments, DSS 2205 exhibits excellent corrosion resistance as a result of chromium and molybdenum enriched passive film. However, the presence of chloride ions in biological solutions may induce localized corrosion, especially pitting corrosion, of metallic biomaterials. In addition, the inflammation process present in the biological system was found to alter local electrochemical parameters and increase hydrogen absorption by DSS 2205, making the alloy vulnerable to hydrogen damage, including stress corrosion cracking (SCC) [7, 8].

Cathodic polarization (CP) is a fundamental electrochemical technique used to study the corrosion behavior and protection mechanisms of metallic alloys. During CP a controlled negative potential is applied to a metallic specimen, lowering the potential to more negative values away from its corrosion potential (E_{corr}) where reduction reactions dominate as the rate of anodic reaction responsible for metal dissolution is decreased [9]. CP can be used to study hydrogen evolution kinetics, cathodic protection conditions, and surface reaction mechanisms that govern corrosion processes in various environments. During CP, the flow of electrons toward the metal surface enhances the reduction reactions. The cathodic reactions depend on the environment to which metals are exposed. For example, in aerated neutral or alkaline solutions, oxygen is reduced to hydroxide ions according to ($O_2 + 2H_2O + 4e^- \rightarrow 4OH^-$), while in acidic solutions, hydrogen reduction occurs according to ($2H^+ + 2e^- \rightarrow H_2$) [10].

Additionally, under CP the passive film of metals including stainless steels may be altered. For instance, the passive film could be stabilized or even repaired leading to enhanced corrosion resistance. It should also be noted that any excessive CP may lead to adverse effects such as hydrogen embrittlement. This would compromise the performance of metals under mechanical loading [11].

The effects of cathodic polarization (CP) as a surface modification technique on the corrosion resistance of DSS 2205 have been reported in the literature. In general, CP alters the composition and characteristics of the passive film, leading to enhanced resistance against both localized and uniform corrosion in this alloy.

For instance, the study by Yan et al.[8] described an electrochemical transient model which was used to study the impact of SCC of 2205 duplex stainless steel at varying polarization potential values. Their findings indicated that higher negative potentials promoted hydrogen-induced damage resulting in the breakdown of the passive film, reduction in repassivation ability, and SCC. At −850 mV (SCE), the interaction between anodic dissolution and hydrogen embrittlement resulted in the formation of severe pits and SCC.

The effect of hydrogen embrittlement on 2205 duplex stainless steel was investigated by Zucchi et al. [12] using slow strain rate testing in acidified artificial seawater. The authors found that hydrogen embrittlement increased with cathodic polarization and sulphide ion concentration, while the formation of a calcareous deposit at highly negative potentials reduced susceptibility to cracking.

The effect of hydrogen on the mechanism of passivation and SCC of 2205 duplex stainless steel in acidified sea water was studied by Pan et al. [13] Hydrogen was found to destabilize the passive film, promote localized anodic dissolution, and increase SCC tendency via hydrogen embrittlement and facilitated anodic dissolution. Cracking was initiated in the ferritic region and proceeded via trans-granular and inter-granular mechanisms

Yang et al. [14] studied the influence of secondary passivation on the passive film of 2205 duplex stainless steel was studied by electrochemical and surface analysis methods. The authors found that secondary passivation increased the pitting corrosion resistance of the material by increasing the compactness of the passive film, decreasing its defect density, and preventing the adsorption and diffusion of chloride and sulfate ions into the film.

Although cathodic polarization has been widely studied regarding its effects on hydrogen embrittlement and stress corrosion cracking in 2205 Duplex Stainless Steel, the impact of such conditions on the electrical properties of the passive layer in physiological environments is inadequately researched. The objective of this research is to examine the effect of CP on the behavior of passive film and corrosion resistance of DSS 2205 in 0.9% wt. NaCl solution. The study seeks to investigate how CP affects the stability, semiconductor properties and barrier effectiveness of passive film as well as changes in corrosion resistance. The effect of CP on the electrochemical kinetics parameters such as charge transfer resistance (R_{ct}), donor density (ND), and flat-band potential (V_{fb}) was examined to identify the influence of such treatment on the corrosion resistance of DSS 2205.

Experimental Procedure

Material Preparation and Characterization

The material used in this research was cut from a plate of DSS 2205. The chemical composition (in mass fractions, wt %) is 22 Cr, 5.5 Ni, 3.2 Mo, 0.18 N, 0.03 C, 0.03 P, 0.02 S, and Fe (balance). For microstructure analysis and electrochemical tests, square samples with area of 1 cm² were precisely cut using a manual bench shear then mounted in epoxy resin. For electrochemical testing and prior to mounting, a copper wire was soldered to one side of each sample.

All samples were then mechanically polished with set of SiC papers down to 1200 grit then polished using a 3-micron diamond paste to remove surface irregularities, followed by fine polishing with 0.5-micron alumina to create a mirror-like smooth surface free of scratches. To study the microstructure, a polished sample was etched with Carpenter's solution (15

mL HCl and 85 mL ethanol) and observed using a Leica optical microscope.

The hardness of DSS 2205 was measured using a Digital Vickers Hardness tester (Figure 1) using a diamond pyramid indenter. The micro hardness tester was calibrated using a standard reference sample. A load of 0.5 kgf (4.90N) was applied for a dwell time of 10 seconds. To ensure reproducibility, multiple indentations were made at different locations and the average hardness value is reported here.

Figure 1: Digital Vickers Hardness Meter

Electrochemical Testing

EIS and MS analysis, were conducted using a by immersing the samples in naturally aerated and stagnant 0.9 wt.% NaCl (Normal saline) solution simulating physiological environment. Electrochemical tests were carried out in a three electrodes electrochemical cell configuration. As shown in Figure 2, the sample, graphite rod, and a silver/silver chloride (Ag/AgCl) electrode served as the working, counter, and reference electrode, respectively.

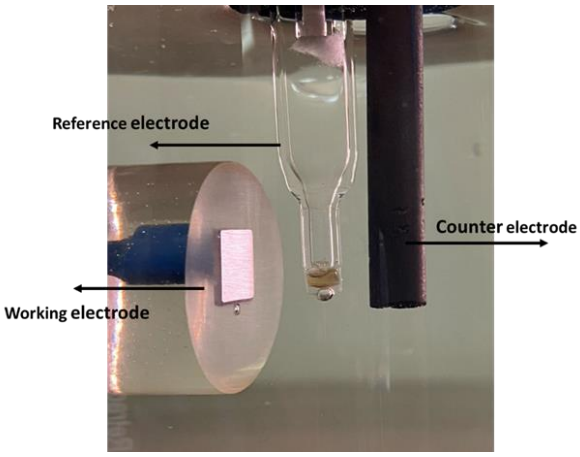

Figure 2: Three electrode electrochemical cell configuration

To study the electrochemical behavior of the alloy with no CP treatment, EIS was performed after allowing the sample to stabilize in the electrolyte for 3600 seconds hence establish a steady E_{OC}. MS analysis was then conducted to evaluate the semiconducting properties of the passive film. To investigate the effect of CP (simulate a cathodic condition), a potential of -400 mV vs. E_{OC} was applied for 1800 seconds. After which, the system was allowed to re-establish its equilibrium condition at E_{OC} for 3600 seconds. Finally, EIS and MS measurements were performed.

EIS tests were used to study the impedance behavior of the passive film. The frequency range was from 100 KHz to 0.01 Hz measured at 5 points per decade. A sine-wave AC voltage of 10 mV_{rms} was applied with a DC voltage of 0 V versus E_{OC}. The semiconducting behavior of the passive film was studied using MS analysis. The potential was swept between 0 V and 0.3 V vs E_{OC} with a voltage amplitude of 10 mV_{rms}, sweep rate of 0.01 V, and frequency of 1 KHz.

All electrochemical tests were conducted at room temperature. Electrochemical test data were obtained through the Gamry Framework software by linking the Gamry potentiostat to a computer (Figure 3). Data was then fitted and analyzed using Gamry E-chem Analyst software. To ensure data reproducibility and accuracy, the results of three samples for each electrochemical test are reported.

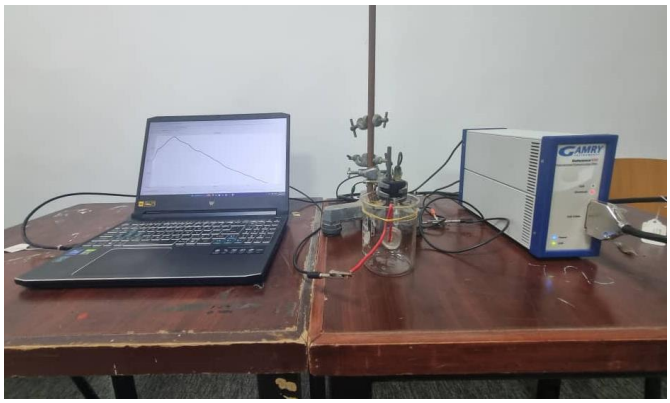

Figure 3: Data acquisition setup

Results and Discussion

Microstructure

As shown in Figure 4, the microstructure of DSS 2205 is composed of almost equal amounts of ferrite (alpha phase) and austenite (gamma phase) at about 50% each. The light regions represent the ferrite matrix which is the base structure, and the dark etched regions are the austenitic phase creating islands or elongated grains within the ferrite matrix. The dual-phase microstructure of duplex stainless steel provides an excellent combination of mechanical properties. The ferrite phase, which has a body-centered cubic (BCC) crystal structure and is enriched in chromium and molybdenum, provides high strength and enhanced resistance to chloride-induced stress corrosion cracking. In contrast, the austenite phase, which possesses a face-centered cubic (FCC) crystal structure and is enriched in nickel and nitrogen, contributes superior toughness, ductility, and localized corrosion resistance [15]. The balanced distribution of these two phases is responsible for the excellent combination of mechanical properties and corrosion resistance exhibited by 2205 duplex stainless steel. Maintaining an appropriate ferrite–austenite balance is essential, as excessive heat treatment or improper cooling can promote the formation of deleterious secondary phases, such as sigma phase, which may significantly reduce both corrosion resistance and mechanical toughness.

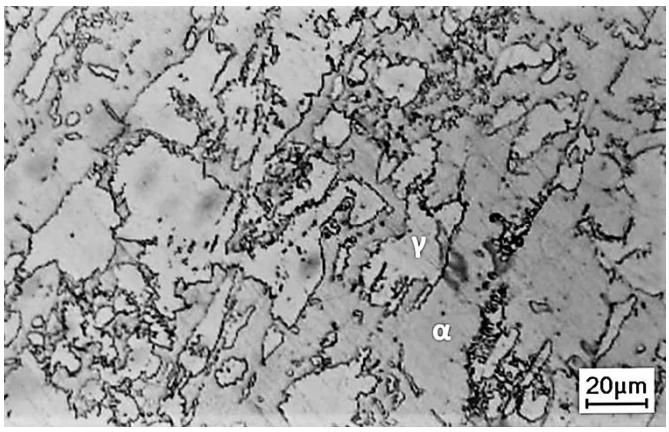

Figure 4: Microstructure of DSS 2205.

Electrochemical Tests

To evaluate the effect of CP on the electrochemical kinetics at the sample-electrolyte interface, EIS measurements were conducted in normal saline solution. The Nyquist diagram for representative results is shown in Figure 5 comparing the case without (a) and with (b) CP. In general, the size of the diameter provides indication of the corrosion resistance of the alloy through R_{CT}.

The plots in the diagram were generally similar in having a single capacitive loop shape, indicating the formation of a protective passive film on the metal surface. The single capacitive loop observed in the Nyquist plots usually signals that one effective time constant dominates the measured frequency range, often linked to charge-transfer plus double-layer (or CPE) behavior. Compared with the specimen without cathodic polarization (Figure 5.a), the application of cathodic polarization (Figure 5.b) resulted in a smaller capacitive semicircle, indicating a decrease in polarization resistance. This behavior suggests deterioration of the passive film and a consequent reduction in the corrosion resistance of DSS 2205.

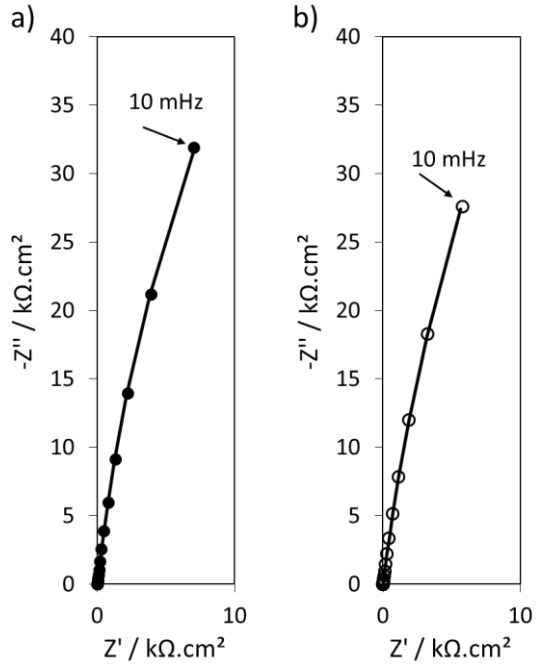

Figure 5: Representative Nyquist plots of 2205 DSS in normal saline solution, (a) without CP and, (b) with CP

The experimental data were interpreted using the analog equivalent circuit model shown in Figure 6. This simplified Randles cell includes a solution resistance (Rs), a double layer capacitor in the form of constant phase element (CPE) in parallel with the charge transfer resistance (R_{CT}). The CPE represents non-ideal capacitive behavior caused by distributed kinetics or structural/energetic heterogeneity at electrochemical interfaces. [16]. In practice, CPEs are introduced whenever simple RC circuits cannot fit impedance data, especially for real double layers, films, porous or rough electrodes, and energy-storage devices [17].

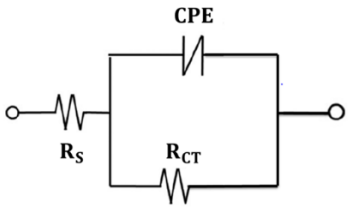

Figure 6: Equivalent circuit model

The impedance of the non-ideal capacitance CPE is represented as:

$$Z_{CPE} = Y_o^{-1}(j\omega)^{-n}, \qquad (1)$$

where Yo is a constant representing a base admittance, j = $(-1)^{1/2}$, ω is the angular frequency, and n is a frequency dependence exponent which measures the deviation from ideal capacitor behavior. The values of n are between 0 and 1. The CPE reduces to a simple capacitor with $C=Y_O$ when n=1. The numeric value of Y_O is roughly indicative of an effective interfacial capacitance, disregarding dimensional issues. As shown in **Error! Reference source not found.**, the fitted results (solid lines) closely matched the experimental behavior for almost all of the frequency range for all results.

There Rs of all electrolytes was in the range of 25 ± 4 Ω.cm^2. As expected, the values are consistent with the cell dimensions and electrolyte resistivity and independent of the material tested and electrolyte type. It should be noted here that when the R_{CT} is much larger than the Rs, the later will not appear in Nyquist plots.

Error! Reference source not found. and Table 1 show the values of the parameters of the CPE elements (n and Y_O) obtained from fitting EIS data with the equivalent circuit shown in **Error! Reference source not found.**.

Y_O shown in Figure 7.a, represents a reasonable indication of the surface roughness or heterogeneity of the passive film. In general, higher values suggest a more defective or porous passive film. The values of Y_O were found to be nearly the same in both conditions, with only a very slight increase under CP condition. These results suggest that cathodic polarization has little influence on the surface heterogeneity and capacitive characteristics of the passive film formed on DSS 2205. Although a slight increase was observed following polarization, the values remain within the experimental error range, indicating that any changes to the passive film are relatively minor.

Error! Reference source not found. (b) shows the effect of CP on the parameter (n). This parameter indicates the capacitive behavior defined by the surface inhomogeneity of the steel at the interface with the electrolyte. i.e., how closely the electrochemical interface behaves like an ideal capacitor. In both conditions (n) values were found to be close to 1, indicating a nearly ideal capacitive behavior.

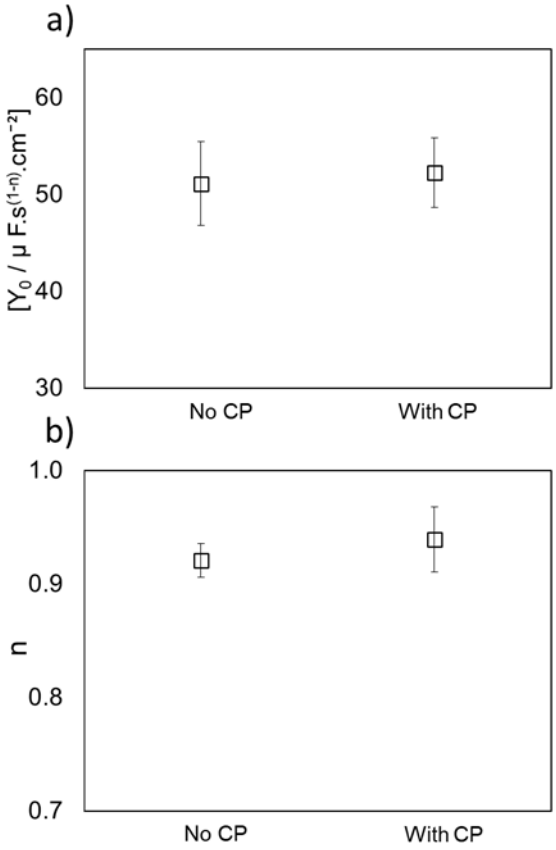

Figure 7: Effect of CP on the magnitudes derived from EIS tests (a) Yo, (b) n, of DSS 2205 after immersion in normal saline. The error bars represent the standard deviation of data.

The values of n remained close to unity under both conditions, indicating near-ideal capacitive behavior of the passive film. In general, an increase in the CPE exponent n suggests that the interface behaves more like an ideal capacitor, reflecting a reduced dispersion of time constants and lower surface or transport heterogeneity. Therefore, the slight increase in n observed after the application of CP may indicate a marginal improvement in the capacitive response of the passive film, possibly due to a more homogeneous passive layer at the metal–solution interface.

As (n) approaches the value of 1, the CPE parameter Y_O may be viewed as a rough estimate of the film capacitance C via

$$C = Y_o . sec^{n-1}, \qquad (2)$$

recognizing that the expression becomes increasingly inaccurate as (n) decreases from unity. A nominal thickness of the passive film (d) may be obtained from the following equation [18]

$$d = \varepsilon\varepsilon_o A/C, \qquad (3)$$

where ε is the dielectric constant of the passive film (taking it to be ~15.6 for stainless steel, ε_o is the permittivity of vacuum (8.85×10^{-14} F.cm^{-1}) and A is the exposed surface area (~1 cm^2).

Under both conditions (with and without CP), the calculated thickness of the passive film was found to be ~ 1.9 nm indicating that CP had no measurable effect on the passive film thickness of DSS 2205 in normal saline solution. This value is comparable with values reported in the literature for oxide films formed on 2205 DSS under various environmental conditions. [19, 20]. It can be concluded here that CP did not affect the integrity and compactness of the passive film where the influence of CP did not penetrate or disrupt the physical structure of the oxide film.

MS technique is a very useful electrochemical tool used to study semiconductor – electrolyte interface properties such as Vfb, ND, and space charge. In the anodic region MS experiment analyzes the behavior of the alloy under oxidative condition which is very important in corrosion studies. In the anodic region a positive potential is applied to the semiconductor electrode creating either hole accumulation (in p type) or depletion (in n type). In the MS analysis the capacitance (C) is measured as a function of applied potential (V) in a plot of $1/C^2$ vs. V. A linear trend in this plot indicates MS behavior which in turn allows for determining the V_{fb} from the x-axes intercept and the donor/acceptor density from the slope of the line [21]. To minimize errors, high-frequency AC impedance of 1 kHz was used in this work.

During MS test, the charge distribution at the semiconductor/solution could be measured by calculating the electrode capacitance [22]:

$$\frac{1}{C^2} = \frac{2}{\varepsilon\varepsilon_0 e N_d}(E - E_{fb} - \frac{KT}{e}) \qquad (4)$$

For n-type semiconductor

$$\frac{1}{C^2} = \frac{-2}{\varepsilon\varepsilon_0 e N_a}(E - E_{fb} - \frac{KT}{e}) \qquad (5)$$

For p-type semiconductor

where C is the capacitance, ε is the dielectric constant of the passive film (15 for stainless steel [23]), ε_o is the permittivity of vacuum (8.85×10^{-14} Fcm^{-1}), Nd and Na are the donor and acceptor densities respectively, E is the applied potential, E_{fb} is the flat band potential, K is Boltzmann constant (1.38×10^{-23} JK^{-1}), T is the absolute temperature, and e is the elementary charge (1.602×10^{-19} C).

Figure 8 shows the results of MS analysis of DSS 2205 in normal saline solution comparing between CP and no CP conditions. For the case of without CP, the linear MS plot was found to displayed n-type semiconductor behavior (as in equation 4) with a positive V_{fb} and low ND. This passive film with n-type semiconductor behavior exhibits selective transport properties that favor anion transport in solution, thereby hindering the mobility of metal cations from stainless steel through the passive film into the electrolyte [24]. Under both conditions, the carrier density was in the range of 10^{20} cm^{-3}, in agreement with the results of other studies [20, 24, 25].

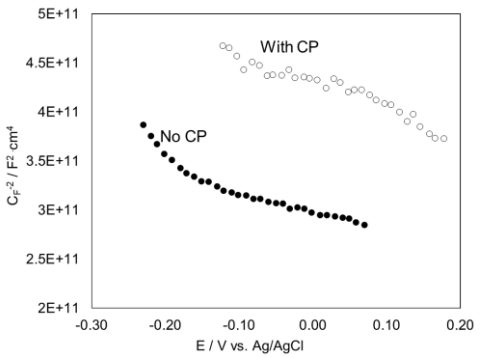

Figure 8: MS plots of passive films formed on DSS 2205 in normal saline solution without cathodic polarization (NO CP) and with cathodic polarization (With CP)

The V_{fb} is critical parameter that can be used for determining the location of semiconductive energy bands with respect to the redox potentials of electro-active ions present in solutions, thus defining passive film stability [20, 24, 26]. As shown in Figure 9.a and listed in Table 1, MS analysis showed a significant difference in the behavior of the passive film of DSS 2205 under CP and no CP conditions. The V_{fb} of the alloy decreased from about –0.05 V vs. Ag/AgCl to about –0.08 Vvs. Ag/AgCl due to application of CP, suggesting the deterioration of the electronic properties of the passive film stability [26].

Figure 9.b and Table 1 show a variation in carrier ND of DSS 2025 in normal saline solution under no CP (ND = 1.6×10^{20} cm^{-3}) and no CP (ND = 3.6×10^{20} cm^{-3}) conditions. The increase in carrier density under CP could be attributed to changes in the electronic structure of the passive film. The oxygen vacancies and other defects may act as donor sites within the oxide film. In general, the higher ND indicates a less protective passive film, as these defects facilitate charge transport through the passive film and provide pathways for corrosive species to penetrate the oxide layer [20, 27].

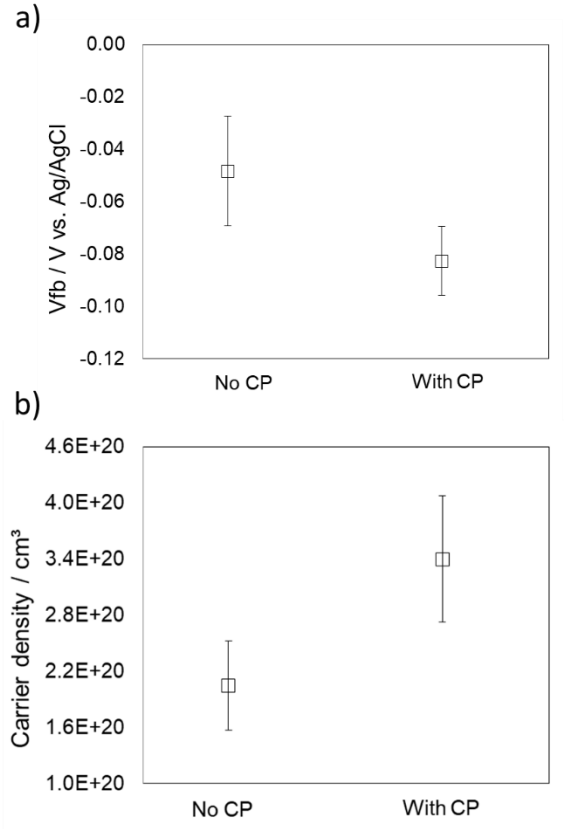

Figure 9: Effect of CP on (a) Vfb, (b) Nd of DSS 2205 after immersion in normal saline. The error bars represent the standard deviation of data.

Table 1: Electrochemical parameters from EIS and MS tests of 2205 DSS in 0.9% wt. NaCl. Values shown as average ±standard deviation.

	Y_O x10^{-6}	n	V_{fb}	MD x10^{20}
	$F.s^{(1-n)}.cm^{-2}$		V	cm^{-3}
No CP	51.3 ±4.3	0.92 ±0.01	-0.05 ±0.018	1.6 ±0.47
CP	53.5 ±3.6	0.94 ±0.02	-0.08 ±0013	3.6 ±0.67

The increase in ND can be related to hydrogen uptake during cathodic polarization. Hydrogen uptake can lead to degradation of the oxide layer by thinning the protective passive film and increasing the number of defects in the oxide layer for super duplex stainless steel [28]. The greater the hydrogen uptake, the thinner the passive film will become and may eventually lose its protective nature[29]. Under strong cathodic polarization, surface oxides on stainless steels are thermodynamically unstable; hydrogen absorption drives a reduction sequence of Fe and Cr oxides that thins the Cr_2O_3-rich passive layer and progressively destroys passivity [28, 30].

A correlation between the different results under both conditions (CP and no CP) indicated that hardness and ND increased simultaneously, while both were associated with a decrease in the V_{fb}. A similar trend was observed in the EIS derived parameters Y_O and n, suggesting the modification of the electrochemical characteristics of the passive film due to CP. Although, the changes in the above-mentioned parameters may indicate a correlated alteration of the passive film following CP, since only two experimental conditions were evaluated, these observations should be considered as qualitative trends not statistically significant correlations.

Conclusions

The effect of cathodic polarization (CP) on the passive film electronic properties and corrosion resistance of DSS2205 stainless steel in normal saline solution was investigated. The increase in donor density (ND) is associated with hydrogen uptake during CP, which increases oxide defects and thins the passive film, thereby reducing its protective effectiveness. The negative shift in flat band potential indicated the deterioration of the electronic properties of the passive film.

The corrosion resistance of the alloy was decreased as indicated by the reduced charge transfer resistance to ~ 30 $k\Omega\cdot cm^2$ under CP, which did not affect the thickness of the passive film of ~ 1.9 nm. Hydrogen ingress was found to modify the electronic properties of the passive film without altering its structure leading to acceleration in local corrosion. While CP does a good job at reducing general corrosion it also brings in issues like hydrogen embrittlement and passive film destabilization. Use of Electrochemical Impedance Spectroscopy (EIS) along with Mott-Schottky (MS) analysis provides that which is very useful in that it links the macro scale impedance changes to the nano scale semiconductor behavior of the passive film.

Author Contributions: Mraied: contributed to conceptualization, methodology, validation, formal analysis, investigation, writing original draft, writing review and editing, visualization, supervision, and project administration; **Alezmirly** and **Almahrug**: contributed to investigation, writing original draft, formal analysis, and visualization. All authors reviewed and approved the final version of the manuscript.

Funding: "This research received no external funding."

Data Availability Statement: "The data are available at request."

Acknowledgments: "The authors would like to express their appreciation to the Advanced Occupational Center for Welding Technologies."

Conflicts of Interest: "The authors declare that they have no conflict of interest."

References

[1] Higelin, S. Le Manchet, and G. Passot, "Heat-affected zone ferrite content control of a duplex stainless steel grade to

enhance weldability," *Weld World*, vol. 66, pp, 1503–1519, 2022. https://doi.org/10.1007/s40194-022-01326-0

[2] Y. Han, Z. Liu, C. Wu. et al. "A short review on the role of alloying elements in duplex stainless steels," *Tungsten*, vol. 5, pp, 419–439, 2023. https://doi.org/10.1007/s42864-022-00168-z

[3] O. Olaseinde, "Comparative Study of the Effect of Temperature on the Corrosion Behaviour of 2205 Duplex Stainless Steel and 316 Austenitic Stainless Steel in Acidic Chloride Environment," *Advances in Materials Physics and Chemistry*, vol. 5, no. 1, pp, 185-190, 2015. https://doi.org/10.4236/ampc.2015.55019.

[4] G. Ran, W. Tu, H. Dong, et al. "Comparative statistical analysis of pitting in Two 2205 duplex stainless steel variants," *npj Mater Degrad*, vol. 8, no. 30 pp, 1-16, 2024. https://doi.org/10.1038/s41529-024-00448-8

[5] J. Tang, X. Yang, Y. Wang, et al. "Corrosion Behavior of 2205 Duplex Stainless Steels in HCl Solution Containing Sulfide," *Metals*, vol. 9, no. 3, pp, 294-300, 2019. https://doi.org/10.3390/met9030294

[6] S.Kim, S.Park, M.Gu, et al. "Chloride-Induced Stress Corrosion Cracking Behavior of Duplex Stainless Steels for Dry Storage Canister Application Via Atmospheric Corrosion Tests and Scanning Electrochemical Microscopy," *ECS Meeting Abstracts*, vol. MA2024-02, no. 17, p, 1708, 2024. https://doi.org/10.1149/MA2024-02171708mtgabs

[7] A. Sharfeddin, H. Mraied, and E. Trok, "Corrosion resistance of 2205 duplex stainless steel in normal saline solution under simulated inflammatory conditions," *Journal of Engineering Research*, vol. 36, pp, 69-80, 2023. https://doi.org/10.66411/jer.v36i.53

[8] Y. Pan, B. Sun, H. Chen, et al. "Stress corrosion cracking behavior and mechanism of 2205 duplex stainless steel under applied polarization potentials," *Corrosion Science*, vol. 231, p, 111978, 2024. https://doi.org/10.1016/j.corsci.2024.111978

[9] C. Googan, "The cathodic protection potential criteria: Evaluation of the evidence," *Materials and Corrosion*, vol. 72, no. 3, pp, 446-464, 2020. https://doi.org/10.1002/maco.202011978

[10] Y. Yao, J. Xu, and M. Shao, "Competitions between hydrogen evolution reaction and oxygen reduction reaction on an Au surface," *Chinese Journal of Catalysis*, vol. 73, pp, 271-278, 2025. https://doi.org/10.1016/S1872-2067(25)64650-X

[11] D. Sobola, and R. Dallaev, "Exploring Hydrogen Embrittlement: Mechanisms, Consequences, and Advances in Metal Science," *Energies*, vol. 17, no. 12, p. 2972, 2024. https://doi.org/10.3390/en17122972

[12] F. Zucchi, V. Grassi, C. Monticelli, and G. Trabanelli, "Hydrogen embrittlement of duplex stainless steel under cathodic protection in acidic artificial sea water in the presence of sulphide ions," *Corrosion Science*, vol. 48, no. 2, pp, 522-530, 2006. https://doi.org/10.1016/j.corsci.2005.01.004

[13] Y.Pan, B.Sun, Z.Liu, et al. "Hydrogen effects on passivation and SCC of 2205 DSS in acidified simulated seawater," *Corrosion Science*, vol. 208, p. 110640, 2022. https://doi.org/10.1016/j.corsci.2022.110640

[14] G.Yang, Y.Du, S.Chen, et al. "Effect of secondary passivation on corrosion behavior and semiconducting properties of passive film of 2205 duplex stainless steel," *Journal of Materials Research and Technology*, vol. 15, p, 6840, 2021. https://doi.org/10.1016/j.jmrt.2021.11.118

[15] R. Francis, and G. Byrne, "Duplex stainless steels—alloys for the 21st century," *Metals*, vol. 11, no. 5, p. 836, 2021. https://doi.org/10.3390/met11050836

[16] H. Mraied, and W. Cai, "The effects of Mn concentration on the tribocorrosion resistance of Al–Mn alloys," *Wear*, vol. 380-381, pp. 191-202, 2017. https://doi.org/10.1016/j.wear.2017.03.017

[17] A. Lasia, "The Origin of the Constant Phase Element," *The journal of physical chemistry letters*, vol. 13, no. 52: pp. 580-589, 2022. https://doi.org/10.1021/acs.jpclett.1c03782

[18] Y.Li, Y.Zhang, Y.Tang, et al. "Hydrogen induced degradation mechanism of passive film in 2205 duplex stainless steel," *Journal of Materials Research and Technology*, vol. 42, pp. 168-177, 2026. https://doi.org/10.1016/j.jmrt.2026.03.114

[19] J. Yao, D. Macdonald, and C. Dong, "Passive film on 2205 duplex stainless steel studied by photo-electrochemistry and ARXPS methods," *Corrosion Science*, vol. 146, pp. 221-232, 2019. https://doi.org/10.1016/j.corsci.2018.10.020

[20] H. Luo, C.F. Dong , K. Xiao, X.G. Li, "Characterization of passive film on 2205 duplex stainless steel in sodium thiosulphate solution," *Applied Surface Science*, vol. 258, no. 1, pp. 631-639, 2011. https://doi.org/10.1016/j.apsusc.2011.06.077

[21] A.Hankin, F. Bedoya-Lora, J. Regoutz, and G. Kelsall, "Flat band potential determination: avoiding the pitfalls," *Journal of Materials Chemistry A*, vol. 7, no. 45, pp. 26162–26176, 2019. https://doi.org/10.1039/C9TA09569A

[22] S. Choi, Y. Yoo, and Y. Kim, "Dynamic Variation in the Semiconductive Tendency of the Passive Film on Duplex Stainless Steel in Corrosion Environments," *Materials*, vol. 17, no. 23, p. 5963, 2024. https://doi.org/10.3390/ma17235963

[23] A. Fattah-alhosseini, and S. Vafaeian, "Passivation behavior of a ferritic stainless steel in concentrated alkaline solutions," Journal of Materials Research and Technology, vol. 4, no. 4, pp. 423, 428, 2015. https://doi.org/10.1016/j.jmrt.2015.02.003

[24] Y.Li, S.Zhu, J.Xian, X.Li, et al. "Electrochemical behavior of 2205 duplex stainless steel in simulated solution containing high concentration Cl− and saturated CO2 at different temperatures," *Scientific Reports*, vol. 12, no. 1, p. 11822, 2022. https://doi.org/10.1038/s41598-022-16096-4

[25] H.Luo, C. F. Dong, X. Q. Cheng, et al. "Electrochemical Behavior of 2205 Duplex Stainless Steel in NaCl Solution with Different Chromate Contents," *Journal of Materials Engineering and Performance*, vol. 21, no. 7, pp. 1283-1291, 2012. https://doi.org/10.1007/s11665-011-0030-1

[26] I. Ogunsanya, C. Hansson, "The semiconductor properties of passive films and corrosion behavior of stainless steel reinforcing bars in simulated concrete pore solution," *Materialia*, vol. 6, no. 2, p. 100321, 2019. https://doi.org/10.1016/j.mtla.2019.100321

[27] L. Zeng, X.P. Guo b, et al. "Semiconductivities of passive films formed on stainless steel bend under erosion-corrosion conditions," *Corrosion Science*, vol. 144, pp. 258-265, 2018. https://doi.org/10.1016/j.corsci.2018.08.045

[28] C. Örnek, F. Zhang, A. Larsson, et al. "Understanding Passive Film Degradation and its Effect on Hydrogen Embrittlement of Super Duplex Stainless Steel – Synchrotron X-Ray and Electrochemical Measurements Combined with Calphad and Ab-Initio Computational Studies," *SSRN Electronic Journal*, vol. 628, p. 157364, 2023. https://doi.org/10.1016/j.apsusc.2023.157364

[29] K. Zhang, L. Wu, Z. Zhou, et al. "Effects of hydrogen on passivation and semiconductive properties of passive film on Fe-based amorphous coatings," *Applied Surface Science*, vol. 635, p. 157754, 2023. https://doi.org/10.1016/j.apsusc.2023.157754

[30] P. Schmuki, S. Virtanen, H. S. Isaacs, et al. "Electrochemical Behavior of Cr_2O_3 / Fe_2O_3 Artificial Passive Films Studied by In Situ XANES," *Journal of The Electrochemical Society*, vol. 145, no. 3, pp. 791-801, 1998. https://doi.org/10.1149/1.1838347